

**This is a self-archived version of an original article. This version may differ from the original in pagination and typographic details.**

**Author(s):** Tonev, D.; de Angelis, G.; Deloncle, I.; Goutev, N.; De Gregorio, G.; Pavlov, P.; Pantaleev, I.L.; Iliev, S.; Yavahchova, M.S.; Bizzeti, P.G.; Demerdjiev, A.; Dimitrov, D.T.; Farnea, E.; Gadea, A.; Geleva, E.; He, C.Y.; Laftchiev, H.; Lenzi, S.M.; Lunardi, S.; Marginean, N.; Menegazzo, R.; Napoli, D.R.; Nowacki, F.; Orlandi, R.; Penttilä, H.; Recchia, F.; Sahin, E.; Singh, R.P.; Stoyanova, M.; Ur, C.A.; Wirth, H.-F.

**Title:** Transition probabilities in 31P and 31S : A test for isospin symmetry

**Year:** 2021

**Version:** Published version

**Copyright:** © 2021 Published by Elsevier B.V. Funded by SCOAP3

**Rights:** CC BY 4.0

**Rights url:** <https://creativecommons.org/licenses/by/4.0/>

**Please cite the original version:**

Tonev, D., de Angelis, G., Deloncle, I., Goutev, N., De Gregorio, G., Pavlov, P., Pantaleev, I.L., Iliev, S., Yavahchova, M.S., Bizzeti, P.G., Demerdjiev, A., Dimitrov, D.T., Farnea, E., Gadea, A., Geleva, E., He, C.Y., Laftchiev, H., Lenzi, S.M., Lunardi, S., . . . Wirth, H.-F. (2021). Transition probabilities in 31P and 31S : A test for isospin symmetry. *Physics Letters B*, 821, Article 136603. <https://doi.org/10.1016/j.physletb.2021.136603>



## Transition probabilities in $^{31}\text{P}$ and $^{31}\text{S}$ : A test for isospin symmetry

D. Tonev<sup>a,\*</sup>, G. de Angelis<sup>b</sup>, I. Deloncle<sup>c</sup>, N. Goutev<sup>a</sup>, G. De Gregorio<sup>d,e</sup>, P. Pavlov<sup>a</sup>, I.L. Pantaleev<sup>a</sup>, S. Iliev<sup>a,1</sup>, M.S. Yavahchova<sup>a</sup>, P.G. Bizzeti<sup>f,g</sup>, A. Demerdjiev<sup>a</sup>, D.T. Dimitrov<sup>a</sup>, E. Farnea<sup>h,i,1</sup>, A. Gadea<sup>j</sup>, E. Geleva<sup>a</sup>, C.Y. He<sup>k</sup>, H. Laftchiev<sup>a</sup>, S.M. Lenzi<sup>h,i</sup>, S. Lunardi<sup>h,i</sup>, N. Marginean<sup>l</sup>, R. Menegazzo<sup>b</sup>, D.R. Napoli<sup>b</sup>, F. Nowacki<sup>m</sup>, R. Orlandi<sup>n</sup>, H. Penttilä<sup>o</sup>, F. Recchia<sup>h,i</sup>, E. Sahin<sup>p</sup>, R.P. Singh<sup>q</sup>, M. Stoyanova<sup>r</sup>, C.A. Ur<sup>s</sup>, H.-F. Wirth<sup>t</sup>

<sup>a</sup> Institute for Nuclear Research and Nuclear Energy, Bulgarian Academy of Sciences, BG-1784, Sofia, Bulgaria

<sup>b</sup> INFN, Laboratori Nazionali di Legnaro, I-35020 Legnaro, Italy

<sup>c</sup> CSNSM, CNRS/Université, Paris-Sud XI, 91405 Orsay Campus, France

<sup>d</sup> Dipartimento di Matematica e Fisica, Università degli Studi della Campania "Luigi Vanvitelli", I-8110 Caserta, Italy

<sup>e</sup> INFN, Sezione di Napoli, I-80126 Napoli, Italy

<sup>f</sup> Dipartimento di Fisica e Astronomia, Università di Firenze, I-50019 Sesto Fiorentino Firenze, Italy

<sup>g</sup> INFN, Sezione di Firenze, I-50019 Sesto Fiorentino Firenze, Italy

<sup>h</sup> INFN, Sezione di Padova, I-35131 Padova, Italy

<sup>i</sup> Dipartimento di Fisica e Astronomia, Università di Padova, I-35131 Padova, Italy

<sup>j</sup> Instituto de Fisica Corpuscular, CSIC-Universitat de Valencia, E-46980 Valencia, Spain

<sup>k</sup> Department of Nuclear Physics, CIAE, 102413 Beijing, PR China

<sup>l</sup> Horia Hulubei National Institute of Physics and Nuclear Engineering, 077125 Bucharest-Magurele, Romania

<sup>m</sup> Université de Strasbourg, CNRS, IPHC, F-67000, Strasbourg, France

<sup>n</sup> Advanced Science Research Center, JAEA, Tokai, Ibaraki 319-1195, Japan

<sup>o</sup> University of Jyväskylä, FI-40014 Jyväskylä, Finland

<sup>p</sup> Department of Physics, University of Oslo, N-0316 Oslo, Norway

<sup>q</sup> Inter-University Accelerator Center, New Delhi, India

<sup>r</sup> Faculty of Physics, Sofia University, BG-1164, Sofia, Bulgaria

<sup>s</sup> ELI-NP, Bucharest-Magurele, Romania

<sup>t</sup> Fakultät für Physik, Ludwig-Maximilians Universität München, D-85748, Garching, Germany

### ARTICLE INFO

#### Article history:

Received 24 May 2020

Received in revised form 24 June 2021

Accepted 23 August 2021

Available online 25 August 2021

Editor: B. Blank

#### Keywords:

Mirror nuclei

Lifetime measurements

Transition probabilities

Isospin symmetry

Microscopic multiphonon model

### ABSTRACT

Excited states in the mirror nuclei  $^{31}\text{P}$  and  $^{31}\text{S}$  were populated in the 1p and 1n exit channels of the reaction  $^{20}\text{Ne} + ^{12}\text{C}$ , at a beam energy of 33 MeV. The  $^{20}\text{Ne}$  beam was delivered for the first time by the Piave-Alpi accelerator of the Laboratori Nazionali di Legnaro. Angular correlations of coincident  $\gamma$ -rays and Doppler-shift attenuation lifetime measurements were performed using the multi-detector array GASP in conjunction with the EUCLIDES charged particle detector. In the observed B(E1) strengths, the isoscalar component, amounting to 24% of the isovector one, provides strong evidence for breaking of the isospin symmetry in the  $A = 31$  mass region. Self-consistent beyond mean field calculations using Equation of Motion method based on a chiral potential and including two- and three-body forces reproduce well the experimental B(E1) strengths, reinforcing our conclusion. Coherent mixing from higher-lying states involving the Giant Isovector Monopole Resonance accounts well for the effect observed. The breaking of the isospin symmetry originates from the violation of the charge symmetry of the two- and three-body parts of the potential, only related to the Coulomb interaction.

© 2021 Published by Elsevier B.V. This is an open access article under the CC BY license (<http://creativecommons.org/licenses/by/4.0/>). Funded by SCOAP<sup>3</sup>.

The investigation of mirror nuclei along the  $N = Z$  line is of considerable interest since it directly addresses the validity of the

charge symmetry of the nuclear forces and the role of the Coulomb effects on the nuclear structure. In the limit of long wavelengths, where the Siegert theorem holds, the E1 transition operator is purely isovector. If the charge symmetry of the nuclear force is exact, E1 transitions between states of equal isospin are forbidden in  $N = Z$  nuclei and have equal strength in mirror nuclei. Experimental deviations from the two rules above can, therefore, be used

\* Corresponding author.

E-mail address: [dimitar.tonev@inrne.bas.bg](mailto:dimitar.tonev@inrne.bas.bg) (D. Tonev).

<sup>1</sup> Deceased author.

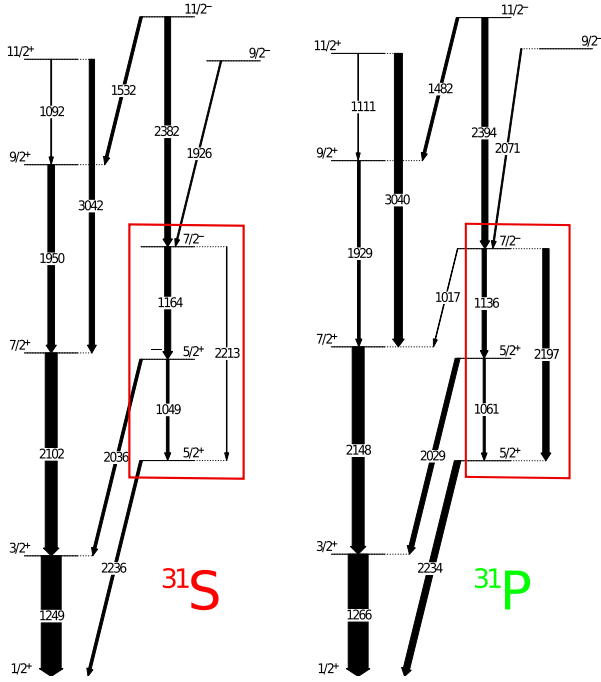


**Fig. 1.** Partial level scheme of  $^{31}\text{S}$  and  $^{31}\text{P}$  from Ref. [1] up to spin  $11/2^-$ . Only the yrast cascades of the two nuclei are shown. The width of the arrows is proportional to the relative intensities of the transitions. The different pattern of the decay of the  $7/2^-$  states in the mirror couple is clearly seen (levels surrounded by rectangles).

to investigate isospin symmetry breaking. The research reported in this paper aims to test the isospin symmetry conservation in the  $A = 31$  region through the comparison of the E1 strengths of the transitions depopulating the  $7/2^-$  analogue states, located slightly above 4400 keV, in the mirror couple nuclei  $^{31}\text{S}$  and  $^{31}\text{P}$  [1]. We show that a beyond mean field and self-consistent approach is able to reach a very good agreement in reproducing the  $B(E1)$  in both nuclei. Fig. 1, reproduced here in a modified form from Ref. [1], shows the partial level schemes of the two mirror nuclei. Mirror E1 transitions  $7/2^- \rightarrow 5/2^-_{1,2}$ , confirmed in the present experiment and indicated with rectangles, clearly show different strengths. In Fig. 1, transition energies and intensities of the  $\gamma$ -rays are taken from the present data set. To verify if the different intensities of those transitions observed in both nuclei correspond to different  $B(E1)$  values, the branching ratios of the transitions de-exciting the states of interest, their M2/E1 mixing ratios and the lifetimes of the two analogue states have to be determined. To achieve this goal angular correlation of coincident  $\gamma$ -rays and Doppler-shift attenuation lifetime measurements have been performed.

Lifetimes of the analogue  $7/2^-$  states in  $^{31}\text{S}$  and  $^{31}\text{P}$  were recently investigated by Pattabiraman et al. [2] using the reaction  $^{16}\text{O} + ^{16}\text{O}$  and utilising Doppler-shift attenuation method (DSAM). In Ref. [2] the lifetime information was obtained gating on  $\gamma$ -rays depopulating a state fed by the level of interest (the so-called ‘‘gate from below’’ method) and making a hypothesis for the unknown feeding of the level, an approach which generally introduces intrinsic uncertainties (the ‘‘gate from below’’ does not exclude feeding from higher-lying long-lived states altering the lifetime measured). Uncertainties on the  $B(E1)$  are even larger if one considers that M2/E1 mixing ratios are generally unknown and one needs to make an assumption on them. In the present experiment the high statistics collected has allowed us to apply, for the lifetime determination using the DSAM procedure, the so-called ‘‘gate from above’’ method, selecting the level of interest gating on the shifted component of the transitions feeding it (therefore excluding unknown feeding from higher-lying states). Multipole mixing ratios

of the transitions of interest were determined performing combined angular correlation analysis based on a large number of angular combinations offered by the GASP multi-detector array. Excited states in  $^{31}\text{S}$  and in  $^{31}\text{P}$  were populated using the  $1n$  and  $1p$  exit channels, respectively, of the reaction  $^{20}\text{Ne} + ^{12}\text{C}$ , at 33 MeV. The beam of  $^{20}\text{Ne}$  was delivered for the first time by the Piave-Alpi accelerator of the Laboratori Nazionali di Legnaro. In order to obtain a thick carbon target needed for a DSAM measurement, we used a two steps procedure. The first step was to evaporate a  $10 \text{ mg/cm}^2$  gold layer on a  $0.6 \text{ mg/cm}^2$   $^{12}\text{C}$  foil. In the second step  $0.15 \text{ mg/cm}^2$   $^{12}\text{C}$  was evaporated onto the carbon foil in order to reach  $0.75 \text{ mg/cm}^2$  final thickness. We noted that this was the maximum carbon thickness we could reach keeping at the same time a high homogeneity of the target. The de-exciting  $\gamma$ -rays were registered with the GASP array [3] in its configuration II. Charged particles were detected with the EUCLIDES silicon ball [4]. Gain matching and efficiency calibration of the Ge detectors were performed using  $^{152}\text{Eu}$  and  $^{56}\text{Co}$  radioactive sources. The data were sorted into coincidence  $\gamma$ - $\gamma$  matrices whereby the detection of protons was required to construct the matrices for  $^{31}\text{P}$ . Angular correlation analyses were performed using the procedure described in the work of Wiedenhöver et al. [5], and with the code CORLEONE. The Ge detectors of the GASP array were grouped into rings according to their polar angles. The relative efficiency of the detector groups was adjusted by requiring a reasonable reproduction of the properties of known  $4^+ \rightarrow 2^+ \rightarrow 0^+$  cascades of the  $^{24}\text{Mg}$ ,  $^{28}\text{Si}$  and  $^{30}\text{Si}$  nuclei also produced in the reaction. An excellent agreement was obtained between the CORLEONE theoretical predictions and the experimental results on  $^{24}\text{Mg}$  and  $^{30}\text{Si}$ , as shown in Ref. [6]. For a given hypothesis, the data analysis consists of fitting the intensity of the cascade by adjusting the parameter  $\sigma$ , characterising the distribution of the magnetic sub-states  $m$  of the spin of the first oriented level, and the multipole mixing ratios  $\delta_1$  and  $\delta_2$  of two consecutive transitions. The analysis was simplified since the spins of the cascade members were known, allowing to optimize only  $\sigma$ ,  $\delta_1$  and  $\delta_2$  parameters.

This procedure was used to derive, from the  $11/2^- \rightarrow 7/2^- \rightarrow 5/2^+$  cascade in  $^{31}\text{S}$  as well as from the  $7/2^- \rightarrow 5/2^+ \rightarrow 3/2^+$  one in  $^{31}\text{P}$ , the multipole mixing ratios for the transitions depopulating the  $7/2^-$  analogue states. Due to the good statistics of the experiment, we constructed 34 detector correlation groups which ensured accurate determination of the multipole mixing coefficients. This number of correlation groups provided data with a statistical significance which mostly eliminates the choice of the background when fitting the spectra. Angular correlation patterns are shown in Figs. 2 and 3. The results for the transitions  $7/2^- \rightarrow 5/2^+$  in both mirror nuclei show a dominant E1 character. The values derived for the M2/E1 multipole mixing ratios are  $\delta = -0.03(7)$  and  $\delta = -0.07(8)$  for  $^{31}\text{P}$  and  $^{31}\text{S}$ , respectively. Our value for  $^{31}\text{P}$ , albeit with a larger error, is in agreement with the previously reported one  $-0.04(3)$  [7]. The  $\delta$  value for the transition in  $^{31}\text{S}$  is measured for the first time and reported in the present Letter. In order to test the sensitivity of the whole procedure, we have compared our results for transitions in  $^{31}\text{P}$  with already known  $\delta$  values and reported in Refs. [7,8]. As an example, the M1/E2 ratio obtained for the  $5/2^+ \rightarrow 3/2^+$  transition of  $+0.04(7)$  is consistent with the previously measured value of  $+0.04(2)$ , reported in the Ref. [7]. Generally, a very good agreement has been found. The second step in our analysis was to derive the lifetimes of the states of interest using the DSAM method. Two related factors are responsible for the determination of the lifetime, respectively for the description of the lineshape, the time evolution of the population of the level of interest and the evolution in time of the velocity distribution of the recoils, starting from the moment of their creation, continuing with their slowing-down in the target and stopper and ending at the moment when they are stopped. To obtain the in-

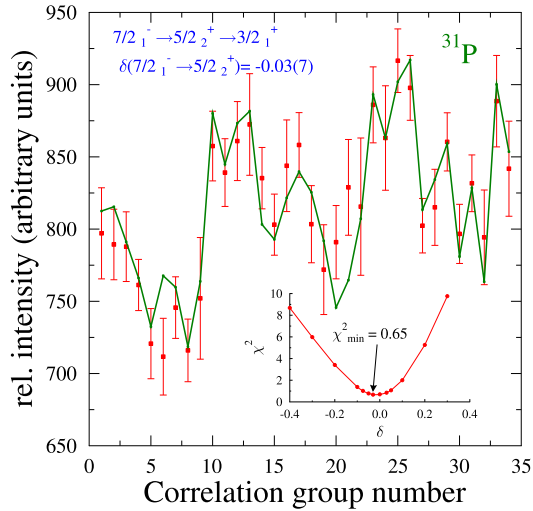


**Fig. 2.** Angular correlation pattern for the cascade involving  $7/2_1^- \rightarrow 5/2_2^+ \rightarrow 3/2_1^+$  transitions of  $^{31}\text{P}$ . Each group number corresponds to a different combination of detectors. The green line is the fit of the data by the CORLEONE code. The quality of the fit ( $\chi^2$ ) as a function of  $\delta$  is shown in the insert of the Figure. The multipole mixing ratio M2/E1  $\delta = -0.03(7)$  obtained for the transition  $7/2_1^- \rightarrow 5/2_2^+$  clearly proves the dominant E1 character of the transition.

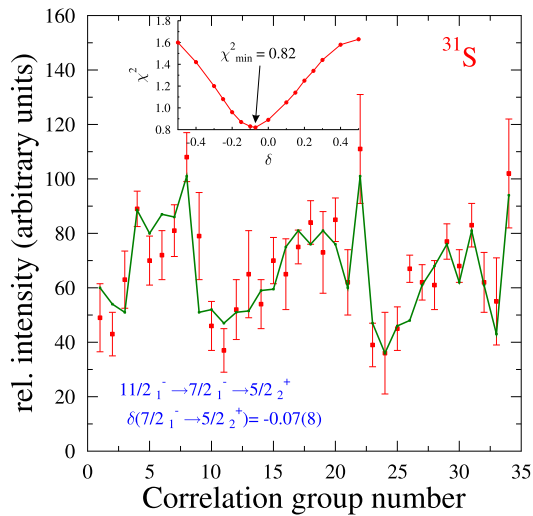


**Fig. 3.** Angular correlation pattern for the cascade involving  $11/2_1^- \rightarrow 7/2_1^- \rightarrow 5/2_2^+$  transitions of  $^{31}\text{S}$ . Each group number corresponds to a different combination of detectors. The green line is the fit of the data by the CORLEONE code. The quality of the fit ( $\chi^2$ ) as a function of  $\delta$  is shown in the insert of the Figure. The multipole mixing ratio M2/E1  $\delta = -0.07(8)$  obtained for the transition  $7/2_1^- \rightarrow 5/2_2^+$  demonstrates the dominant E1 character of the transition.

formation needed we performed a Monte Carlo (MC) simulation of the slowing-down histories of the recoils using a modified version [9,10] of the program DESASTOP [11] written by G. Winter. The electronic stopping powers were taken from the Northcliffe and Schilling tables [12] with corrections for the atomic structure of the medium along the lines discussed in Ref. [13]. As suggested in Ref. [14], an empirical reduction of  $f_n = 0.7$  was applied to down-scale the nuclear stopping power predicted by the theory of Lindhard, Scharff, and Schiött [15]. In order to investigate the impact of the stopping power on the lineshape description we analysed the data using two more approaches: 1) Ward's effective charge and Ziegler's proton stopping power [16–18] and 2) Ziegler's heavy-ion stopping power [18]. All three approaches lead to similar results.

It should also be noted that the derivation of the lifetimes of the mirror states in the same experiment makes the determina-

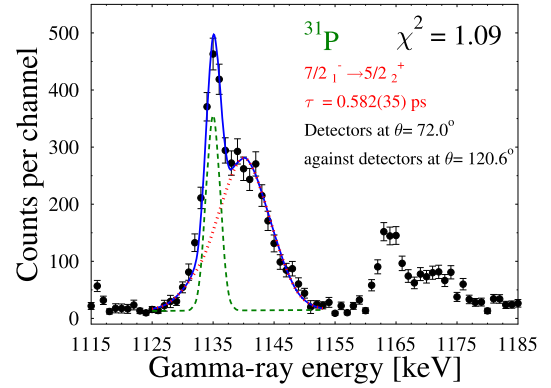


**Fig. 4.** Example of the lineshape analysis of the 1135.6 keV  $\gamma$ -ray transition and determination of the lifetime of the  $7/2_1^-$  in  $^{31}\text{P}$ . The gate is set on a portion of the shifted part of the transition of 2394 keV. The spectrum is measured with the detectors at an angle of  $72.0^\circ$  with respect to the beam axis, the resulting lineshape (full line), the inflight (dotted line) and the unshifted portion (dashed line) fitted components of the transition are presented. The  $\chi^2$  value for the best fit is also indicated.

tion of the ratios of the corresponding transition strengths very precise since uncertainties related to the stopping power nearly cancel. According to our calculations, the mean velocity of the recoils when leaving the target was about 3.7% of the velocity of light and they needed in average 1.1 ps to come to rest. The evaporation of charged particles, which is of importance for the velocity distribution of light residual nuclei, was taken into account in the MC simulation and led to better fits of the spectra [19,20]. Other factors taken into account for the description of the lineshape are: beam energy; reaction; detectors (position, resolution and efficiency); time dependence of the population of the level of interest; relativistic effects etc. Their impact on the systematic error is investigated and taken into account in the final error values of the lifetimes. Additional details on the Monte Carlo simulation can be found in Refs. [9,10,19,21]. The strength of the  $^{31}\text{P}$  and  $^{31}\text{S}$  reaction channels made it possible to apply the procedure for DSAM analysis of coincidence data where the gate is set on the shifted portion of the line shape of a transition directly feeding the level of interest [10]. Within this approach, the timing quality of the gated line shape is improved, compared to the case where the gate includes also fully stopped events that do not provide lifetime information. Moreover, “gating from above” allows the elimination of the uncertainties related to the unobserved feeding of the level of interest which perturbs singles and coincidence measurements when the gate is set on a transition de-exciting a level fed by the level of interest. Fits of the lineshapes obtained in the present work with the procedure described in Ref. [10] and used to determine the lifetimes of the  $7/2_1^-$  states in  $^{31}\text{P}$  and  $^{31}\text{S}$  are presented in Figs. 4 and 5, respectively. (See also the respective captions). It is worth noting that in Ref. [6] this procedure was tested, based on the same data set, extracting the lifetime of the mirror  $3/2_1^+$  states in  $^{31}\text{P}$  and  $^{31}\text{S}$ , for which values are reported in the literature [7,8] and [22]. For the  $3/2_1^+$  state in  $^{31}\text{P}$  our lifetime value of  $\tau = 736(35)$  fs is fully consistent with the value of  $\tau = 745(35)$  fs reported in Ref. [7]. The lifetime determined for the  $3/2_1^+$  state in  $^{31}\text{S}$  of  $\tau = 624(32)$  fs is also consistent with the value previously reported in Ref. [22] of  $\tau = 720(180)$  fs, but it has a smaller error. The lifetime value obtained in the present work for the  $7/2_1^-$  level in  $^{31}\text{P}$  is of  $\tau = 597(45)$  fs, which is in good agreement with the value of  $\tau = 600(100)$  fs reported in [7], but the error we derive is smaller (see Ref. [6]). The value obtained for the  $7/2_1^-$  state of  $^{31}\text{S}$  of  $\tau = 543(49)$  fs is instead in disagreement with that reported in

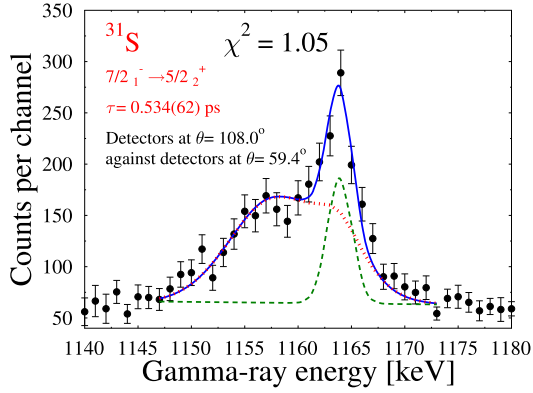


**Fig. 5.** Example of the lineshape analysis of the 1163.9 keV  $\gamma$ -ray transition and determination of the lifetime of the  $I^\pi = 7/2_1^-$  in  $^{31}\text{S}$ . The gate is set on a portion of the shifted part of the transition of 2382 keV. The spectrum is measured with the detectors at an angle of  $108.0^\circ$  with respect to the beam axis, the lineshape (full line), obtained by fitting the broad flight (dotted line) and the narrow unshifted (dashed line) components of the transition are presented. The  $\chi^2$  value for the best fit is also indicated.

Ref. [2] of  $\tau = 1.03(21)$  ps.

By measuring first the branching ratios, multipole mixing ratios and lifetimes we could then determine the  $B(E1)$  values for the two analogue transitions depopulating the  $7/2_1^-$  state of the  $A = 31$  mirror pair. The  $B(E1)$  value derived for the  $7/2_1^- \rightarrow 5/2_2^+$  transition of  $^{31}\text{S}$  is  $B(E1) = 7.2 \times 10^{-4} \pm 0.7 \times 10^{-4} \text{ e}^2 \text{ fm}^2$  which is about two and a half times larger than the value of  $B(E1) = 2.7 \times 10^{-4} \pm 0.2 \times 10^{-4} \text{ e}^2 \text{ fm}^2$  characterising the analogue state in  $^{31}\text{P}$ . For the  $7/2_1^- \rightarrow 5/2_1^+$  transition of  $^{31}\text{S}$  we have only an upper limit but the trend is similar. The results are presented in Table 1. Such a large difference clearly points to a breaking of the isospin symmetry. The breaking term can be expressed by introducing an “induced” isoscalar component in the E1 transition matrix elements, otherwise only isovector. The E1 transition strength can be therefore generally written as a sum of an isoscalar and an isovector term, with the assumption of the former being the smaller.

$$\begin{aligned}
 B(E1) &= \langle J_i; T_i T_3 || \mathcal{M}_{IV} + \mathcal{M}_{IS} || J_f; T_f T_3 \rangle^2 / (2J_i + 1) \\
 &= [(-1)^{1/2-T_3} \begin{pmatrix} 1/2 & 1 & 1/2 \\ -T_3 & 0 & T_3 \end{pmatrix} \times \\
 & \langle J_i; T = 1/2 || \mathcal{M}_{IV} || J_f; T = 1/2 \rangle + \\
 & (-1)^{1/2-T_3} \begin{pmatrix} 1/2 & 0 & 1/2 \\ -T_3 & 0 & T_3 \end{pmatrix} \times \\
 & \langle J_i; T = 1/2 || \mathcal{M}_{IS} || J_f; T = 1/2 \rangle]^2 / (2J_i + 1)
 \end{aligned} \quad (1)$$

For  $T_3 = \pm 1/2$

$$\begin{aligned}
 \begin{pmatrix} 1/2 & 1 & 1/2 \\ -T_3 & 0 & T_3 \end{pmatrix} &= 1/\sqrt{6} \\
 \begin{pmatrix} 1/2 & 0 & 1/2 \\ -T_3 & 0 & T_3 \end{pmatrix} &= (-1)^{1/2-T_3}/\sqrt{2}
 \end{aligned} \quad (2)$$

Using the experimentally determined  $B(E1)$  strength for the couple of  $7/2_1^- \rightarrow 5/2_2^+$  transitions, i.e. 1135.6 keV in  $^{31}\text{P}$  and 1163.9 keV in  $^{31}\text{S}$ , it leads to  $\langle J_i || \mathcal{M}_{IV} || J_f \rangle = 0.149(38)$  efm and  $\langle J_i || \mathcal{M}_{IS} || J_f \rangle = 0.021(2)$  efm. The ratio  $|\langle J_i; T_i T_3 || \mathcal{M}_{IS} || J_f; T_f T_3 \rangle / \langle J_i; T_i T_3 || \mathcal{M}_{IV} || J_f; T_f T_3 \rangle| = |\langle J_i || \mathcal{M}_{IS} || J_f \rangle \sqrt{6} / \langle J_i || \mathcal{M}_{IV} || J_f \rangle \sqrt{2}|$  for the  $7/2_1^- \rightarrow 5/2_2^+$  transitions is then about 0.24. Using the experimental limit of 1% for the branching ratio of the transition 2213 keV  $7/2_1^- \rightarrow 5/2_1^+$  in  $^{31}\text{S}$  we can obtain also a limit for the  $B(E1)$  value. This leads to  $|\langle J_i || \mathcal{M}_{IS} || J_f \rangle \sqrt{6} / \langle J_i || \mathcal{M}_{IV} || J_f \rangle \sqrt{2}|$

$< 0.6$  for the couple of  $7/2_1^- \rightarrow 5/2_1^+$  transitions, i.e. 2197 keV in  $^{31}\text{P}$  and 2213 keV in  $^{31}\text{S}$ , which is consistent with the ratio of 0.24, for the couple of  $7/2_1^- \rightarrow 5/2_2^+$  transitions.

To interpret the results we computed the E1 transition strengths of  $^{31}\text{S}$  and  $^{31}\text{P}$  within the Equation of Motion Phonon Method (EMPM) [23,24] which generates an orthonormal basis of multiphonon states whose constituents are the Tamm-Dancoff Approximation (TDA) phonons. Such a basis is used to diagonalize a Hamiltonian of general form. The method does not rely on any approximation and takes into full account the Pauli principle. We performed a self-consistent calculation using a Hamiltonian composed of an intrinsic kinetic operator and the chiral potential  $\text{NNLO}_{\text{sat}}$  [25], which includes the contribution of the three-body forces. The Hartree-Fock (HF) basis states were generated in a space encompassing all harmonic oscillator shells up to  $N_{\text{max}} = 6$ . The Hamiltonian was diagonalized in a space spanned by an odd hole coupled to TDA phonons. The calculation is completely free of the spurious admixtures induced by the centre of mass motion. They were completely and exactly removed by resorting to the Gram-Schmidt orthogonalization procedure [26].

The wavefunctions are of the form  $|\Psi_\Omega\rangle = \sum_{v_0} C_{v_0}^\Omega |v_0\rangle + \sum_{v_1} C_{v_1}^\Omega |v_1\rangle$  where  $v_0$  is the single hole term and  $v_1 = \sum_{h\lambda} C_{h\lambda}^{v_1} |(h \times \lambda)^{v_1}\rangle$  are the 1-phonon components which arise from diagonalizing the Hamiltonian in the subspace spanned by the states obtained by coupling the hole states ( $h$ ) to the TDA phonons ( $\lambda$ ). These wavefunctions were used to compute the  $B(E1)$  for  $^{31}\text{S}$  and  $^{31}\text{P}$  using the E1 operator with bare charges  $e_p = 1$ ;  $e_n = 0$ . The results obtained are  $B(E1)[7/2_1^- \rightarrow 5/2_1^+] = 7.9 \times 10^{-4} \text{ e}^2 \text{ fm}^2$ ,  $B(E1)[7/2_1^- \rightarrow 5/2_2^+] = 6.9 \times 10^{-4} \text{ e}^2 \text{ fm}^2$  for  $^{31}\text{S}$  and  $B(E1)[7/2_1^- \rightarrow 5/2_2^+] = 2.2 \times 10^{-4} \text{ e}^2 \text{ fm}^2$ ,  $B(E1)[7/2_1^- \rightarrow 5/2_1^+] = 2.4 \times 10^{-4} \text{ e}^2 \text{ fm}^2$  for  $^{31}\text{P}$ . The calculated  $B(E1)$  strengths are in excellent agreement with the experimental ones for the two mirror transitions  $7/2_1^- \rightarrow 5/2_2^+$  and in reasonable accordance (the same order of magnitude) for the  $7/2_1^- \rightarrow 5/2_1^+$ , see Table 1. Following the procedure described above we also get for the couple of  $7/2_1^- \rightarrow 5/2_2^+$  transitions, i.e. 1135.6 keV in  $^{31}\text{P}$  and 1163.9 keV in  $^{31}\text{S}$ ,  $\langle J_i || \mathcal{M}_{IV} || J_f \rangle = 0.147$  efm and  $\langle J_i || \mathcal{M}_{IS} || J_f \rangle = 0.027$  efm, in very good agreement with the experimental data. The calculated  $B(M2)$  values are also reported in Table 1. Using the bare gyromagnetic factors  $g_p = 1$ ,  $g_n = 0$ ,  $g_{sp} = 5.586$  and  $g_{sn} = -3.826$ , we obtain  $B(M2)[7/2_1^- \rightarrow 5/2_1^+] = 6.1 \mu_N^2 \text{ fm}^2$ ,  $B(M2)[7/2_1^- \rightarrow 5/2_2^+] = 1.9 \mu_N^2 \text{ fm}^2$  for  $^{31}\text{S}$  and  $B(M2)[7/2_1^- \rightarrow 5/2_1^+] = 2.5 \mu_N^2 \text{ fm}^2$  and  $B(M2)[7/2_1^- \rightarrow 5/2_2^+] = 2.8 \mu_N^2 \text{ fm}^2$  for  $^{31}\text{P}$ . It is worth pointing out that the violation of the mirror symmetry is here only apparent. In fact, because of the Pauli principle, the proton (neutron) hole couple to the neutron (proton) TDA phonons describing the excitations of the core. The M2 strength comes entirely from the phonons and is larger for protons because of the larger gyromagnetic spin factor and the contribution of the orbital motion.

Different  $B(E1)$  strengths have also been observed in mirror E1 transitions in the  $A = 35$  pair [28] and with opposite phase ( $B(E1)_{T_2=1/2} < B(E1)_{T_2=-1/2}$ ) in the  $A = 67$  couple [29]. As for the mirror pair  $A = 31$ , in both cases ratios  $|\langle J_i || \mathcal{M}_{IS} || J_f \rangle \sqrt{6} / \langle J_i || \mathcal{M}_{IV} || J_f \rangle \sqrt{2}|$  of about 0.30 - 0.40 were found. An extensive discussion on the “isoscalar” term is presented in Ref. [30]. As pointed out there it can have different origins, either related to higher-order terms in the evaluation of the transition operator or to the level mixing induced by the isovector part of the Coulomb interaction. An estimate of the higher-order terms in the transition operator shows that their contribution is small [30] and cannot justify such large values for the ratio. Contributions from mixing with higher-lying levels [2] are, individually, even smaller. Their combined effect, however, can be large if each one of the mixing matrix elements is, to some extent, coherent in phase with the E1 amplitude involving the same level [31]. Most of the contribu-

**Table 1**

Branching ratios, multipole mixing ratios and electromagnetic transition properties. The first section concerns the decay of the  $7/2^-$  state in  $^{31}\text{P}$  with the corresponding lifetime reported, the second one that of the mirror state in  $^{31}\text{S}$ . The first column presents transitions by their initial and final angular momentum and parity assignments  $J_k^\pi$ , the experimental  $\gamma$  energies are given in the second column. The experimentally derived branching ratios, multipole mixing ratio M2/E1, theoretically calculated and experimentally derived values of the B(E1) and B(M2) from the present dataset and B(E1) in Ref. [2] are presented in the following columns.

Transition	$E_f$ (keV)	Br. ratio %	$\delta$	$B(E1)_{th}$ $e^2 \text{fm}^2$	B(E1)	B(E1) [2]	B(M2)	$B(M2)_{th}$ $\mu_N^2 \text{fm}^2$
$^{31}\text{P}$ , $\tau = 597(45)$ fs								
$7/2_1^- \rightarrow 5/2_2^+$	1135.6	37.0(1)	-0.03(7)	$2.2 \times 10^{-4}$	$2.7(2) \times 10^{-4}$	$2.9(5) \times 10^{-4}$	22(11)	2.8
$7/2_1^- \rightarrow 5/2_1^+$	2197.0	58.1(1)	-0.03(3)	$2.4 \times 10^{-4}$	$0.58(4) \times 10^{-4}$	$0.52(4) \times 10^{-4}$	1.3(24)	2.5
$7/2_1^- \rightarrow 7/2_1^+$	1016.4	4.9(1)	-		$0.5(1) \times 10^{-4}$	-	-	
$^{31}\text{S}$ , $\tau = 543(49)$ fs								
$7/2_1^- \rightarrow 5/2_2^+$	1163.9	99(1)	-0.07(8)	$7.9 \times 10^{-4}$	$7.2(7) \times 10^{-4}$	$3.9(8) \times 10^{-4}$	307(+586-307) <sup>a</sup>	1.9
$7/2_1^- \rightarrow 5/2_1^+$	2213.0	< 1(1)	-	$6.9 \times 10^{-4}$	$< 2.2 \times 10^{-4}$	$< 1.15 \times 10^{-6}$	-	6.1

<sup>a</sup> For the 1163.9 keV  $7/2_1^- \rightarrow 5/2_2^+$  transition in  $^{31}\text{S}$ , due to the uncertainties on the  $\delta$  values the B(M2) is numerically ranging from 0 to 80 W.u. To exclude unphysical values we have performed statistical analyses of the B(M2) data compiled in the Nudat files [27], selecting transitions with firmly established E1+M2 multipolarity and energy up to 3 MeV, avoiding less accurate measurements. The resulting mean value of this data set (96 values) is 24 W.u. with a standard uncertainty of 12 W.u. The less probable region is delimited by B(M2) values above 36 W.u. ( $586 \mu_N^2 \text{fm}^2$ ), associated in our case with  $\delta$  lower than -0.097. Correspondingly the evaluated B(M2) value for  $^{31}\text{S}$  is 307 (+586 -307)  $\mu_N^2 \text{fm}^2$ .

tion to the mixing can, therefore, be associated to the isovector giant monopole resonance (IVGMR) built over the state considered [30,32]. The good agreement of our theoretical approach with the experimental data confirms that. The breaking of the isospin symmetry originates from the violation of the charge symmetry of the two- and three-body parts of the chiral potential adopted, which includes the Coulomb interaction. This isospin violating terms, whose detailed discussion can be found in Ref. [33], yield asymmetric wavefunctions and, therefore, asymmetric B(E1) for  $^{31}\text{S}$  and  $^{31}\text{P}$ . Focusing, for instance, on the  $7/2_1^- \rightarrow 5/2_1^+$  E1 transition, the  $5/2_1^+$  state has a single-hole nature while the  $7/2_1^-$  has a hole-phonon structure and contributes to the transition mainly through the component  $(5/2^+(\nu) \times 1_1^-)^{7/2}$  in  $^{31}\text{S}$  and  $(5/2^+(\pi) \times 1_1^-)^{7/2}$  in  $^{31}\text{P}$  (see Refs. [34,35] for details). These components account for the 17% and 7% of the total wavefunctions, respectively. Such an asymmetry generates asymmetric B(E1)'s. In fact, if we turn off all the charge symmetry breaking terms in the interaction and neglect the mass difference between protons and neutrons, we get identical proton and neutron HF and TDA states with equal proton and neutron content (50%) and, consequently, identical spectra, wave functions and transition strengths for the two mirror nuclei.

In summary, our Letter presents a new data set providing detailed information on electromagnetic transition strengths in the mirror nuclei  $^{31}\text{P}$  and  $^{31}\text{S}$ . The comparison of the B(E1) strengths in the two mirror transitions indicates a violation of the isospin symmetry manifested by the presence of a large induced isoscalar component. Self-consistent calculations using the NNLO<sub>sat</sub> and using the Equation of Motion Phonon Method reproduce well the experimental findings, confirming the breaking of the isospin symmetry originating from the violation of the charge symmetry of the two- and three-body parts of the potential. The result provides evidence for a coherent contribution to isospin mixing, probably involving the isovector giant monopole resonance [29]. A microscopic description of the mixing of isospin within the EMPM approach using the isospin formalism for expressing the hole-phonon basis is ongoing.

#### Declaration of competing interest

The authors declare that they have no known competing financial interests or personal relationships that could have appeared to influence the work reported in this paper.

#### Acknowledgements

D.T. expresses his gratitude to Ivanka Necheva and Jordanka Toneva for their outstanding support. Thanks to the PIAVE-ALPI accelerator staff of LNL-INFN, Legnaro, for their excellent work for our experiment. This research has been supported by the Bulgarian Science Fund under Contract No. 08/6, 13.12.2016. A. D. and E. G. are grateful to the *National Post-doctoral students and young scientists* program, funded by the Bulgarian Ministry of Education and Science.

#### References

- [1] D.G. Jenkins, C.J. Lister, M.P. Carpenter, P. Chowdhury, N.J. Hammond, R.V.F. Janssens, et al., Phys. Rev. C 72 (2005) 031303(R).
- [2] N.S. Pattabiraman, D.G. Jenkins, M.A. Bentley, R. Wadsworth, C.J. Lister, M.P. Carpenter, et al., Phys. Rev. C 78 (2008) 024301.
- [3] D. Bazzacco, Chalk River Report AECL 10613, 1992, p. 376.
- [4] E. Farnea, G. de Angelis, M. De Poli, D. De Acuna, A. Gadea, D.R. Napoli, et al., Nucl. Instrum. Methods A 400 (1997) 87.
- [5] I. Wiedenhover, O. Vogel, H. Klein, A. Dewald, P. von Brentano, J. Gableske, et al., Phys. Rev. C 58 (1998) 721.
- [6] D. Tonev, G. de Angelis, P. Petkov, S. Iliev, R. Orlandi, C. Ur, et al., J. Phys. Conf. Ser. 267 (2011) 012048.
- [7] P.M. Endt, Nucl. Phys. A 633 (1998) 1.
- [8] M. Ionescu-Bujor, A. Iordachescu, D.R. Napoli, S.M. Lenzi, N. Marginean, T. Otsuka, et al., Phys. Rev. C 73 (2006) 024310.
- [9] P. Petkov, J. Gableske, O. Vogel, A. Dewald, P. von Brentano, R. Krucken, et al., Nucl. Phys. A 640 (1998) 293.
- [10] P. Petkov, D. Tonev, J. Gableske, A. Dewald, P. von Brentano, Nucl. Instrum. Methods A 437 (1999) 274.
- [11] G. Winter, Nucl. Instrum. Methods 214 (1983) 537.
- [12] L.C. Northcliffe, R.F. Schilling, Nucl. Data. Sect. 7 (1970) 233.
- [13] J.F. Ziegler, J.P. Biersack, in: D.A. Bromley (Ed.), Treatise on Heavy-Ion Science, vol. 6, Plenum Press, New York, 1985, p. 95.
- [14] J. Keinonen, AIP Conf. Proc. 125 (1985) 557.
- [15] J. Lindhard, M. Scharff, H.E. Schiött, Mat.-Fys. Medd. Danske Vid. Selsk. 33 (1963) 14.
- [16] D. Ward, J.S. Forster, H.R. Andrews, I.V. Mitchell, G.C. Ball, W.G. Davies, G.J. Costa, AECL-4914, Chalk River, 1975.
- [17] D. Ward, J.S. Forster, H.R. Andrews, I.V. Mitchell, G.C. Ball, W.G. Davies, G.J. Costa, AECL-5313, Chalk River, 1976.
- [18] J.F. Ziegler, The Stopping and Ranges of Ions in Matter, Vols. 3 and 5, Pergamon Press, 1980.
- [19] D. Tonev, P. Petkov, A. Dewald, T. Klug, P. von Brentano, W. Andrejtscheff, et al., Phys. Rev. C 65 (2002) 034314.
- [20] J.N. Orce, P. Petkov, C.J. McKay, S.N. Choudry, S.R. Lesher, M. Mynk, et al., Phys. Rev. C 70 (2004) 014314.
- [21] D. Tonev, G. de Angelis, S. Brant, S. Frauendorf, P. Petkov, A. Dewald, et al., Phys. Rev. C 76 (2007) 044313.
- [22] R. Engmann, E. Ehrmann, F. Brandolini, C. Signorini, Nucl. Phys. A 162 (1971) 295.

- [23] G. De Gregorio, F. Knapp, N. Lo Iudice, P. Veselý, Phys. Rev. C 94 (2016) 061301(R).
- [24] G. De Gregorio, F. Knapp, N. Lo Iudice, P. Veselý, Phys. Rev. C 95 (2017) 034327.
- [25] A. Ekström, G.R. Jansen, K.A. Wendt, G. Hagen, T. Papenbrock, B.D. Carlsson, C. Forssén, M. Hjorth-Jensen, P. Navrátil, W. Nazarewicz, Phys. Rev. C 91 (2015) 051301(R).
- [26] D. Bianco, F. Knapp, N. Lo Iudice, P. Veselý, F. Andreozzi, G. De Gregorio, A. Porrino, J. Phys. G, Nucl. Part. Phys. 41 (2014) 025109.
- [27] From Evaluated Nuclear Data File, update of 2020-11-04.
- [28] J. Ekman, D. Rudolph, C. Fahlander, A.P. Zuker, M.A. Bentley, S.M. Lenzi, et al., Phys. Rev. Lett. 92 (2004) 132502.
- [29] R. Orlandi, G. de Angelis, P.G. Bizzeti, S. Lunardi, A. Gadea, A.M. Bizzeti-Sona, et al., Phys. Rev. Lett. 103 (2009) 052501.
- [30] P.G. Bizzeti, G. de Angelis, S.M. Lenzi, R. Orlandi, Phys. Rev. C 86 (2012) 044311.
- [31] M. Bini, P.G. Bizzeti, P. Sona, Lett. Nuovo Cimento 41 (1984) 191.
- [32] G. Colo, M.A. Nagarajan, P. Van Isaker, A. Vitturi, Phys. Rev. C 52 (1995) R1175.
- [33] R. Machleidt, D.R. Entem, Phys. Rep. 503 (2011).
- [34] G. De Gregorio, F. Knapp, N. Lo Iudice, P. Veselý, Phys. Rev. C 99 (2019) 014316.
- [35] G. De Gregorio, F. Knapp, N. Lo Iudice, P. Veselý, Phys. Rev. C 101 (2020) 024308.